ISSN 1028-6845

BGJ

BANGLADESH GEOSCIENCE JOURNAL VOL. 24, P. 31-55, 2018

A revisit to the anoxic – oxic evolution of the early Cambrian ocean in the Yangtze Block, South China

RUMANA YEASMIN[1,2*], DAIZHAO CHEN[2] & JIANGUO WANG[2]

Abstract

The dramatic evolution in life form on earth as well as their diversification during the early Cambrian was probably linked to dynamic changes in ocean water chemistry. The ocean water condition during accumulation of the early Cambrian black shale dominant sequences on the Yangtze Block is a widely studied issue, but still debatable. Hence, we compiled different published geochemical data, based on which we tried to construct some paleoenvironmetal models that illustrate the temporal variations of ocean water chemistry of the Yangtze Block during the early Cambrian on a basin scale. By correlating the previously reported Fe-S isotope-trace elements data from inner shelf to deep basin, it has been suggested that the deep ocean waters in the Yangtze Platform was anoxic and ferruginous at the beginning of Cambrian and metastable euxinic waters might have dynamically invaded in shallow shelf waters with an increasing weathering sulfate supply and extended up to upper slope. Evidence for this highly stratified water column is given by increase of istopically lighter sulfur ($\delta^{32}S$) in sedimentary sulfides though the ambient Ediacaran-early Cambrian ocean was depleted in sulfate, high concentrations of reactive iron (Fe) including Fe in sedimentary sulfides, and exceeding contents of redox sensitive trace elements. This stratification of ocean redox chemistry was probably widespread during a marine transgression, but started to shrink and finally, disappeared when the basin evolved with a subsequent regression.

Keywords: Yangtze Block, early Cambrian, anoxia, trace elements, iron speciation, sulfur isotope

Introduction

Soft-bodied Ediacaran fauna started to extinct during Precambrian-Cambrian transition (e.g. NARBONNE, 2005), and were replaced by small shelly fauna (SSFs) during early Cambrian (KNOLL & CARROLL, 1999). This bio-radiation, known as the 'Cambrian Explosion', is one of the most significant periods of animal evolution. Progressive oxygenation of ambient ocean water perhaps prompted this evolutionary diversification (e.g., KNOLL & CARROLL, 1999; SCOTT *et al.* 2008) as seen in late Neoproterozoic when the rise of the atmospheric oxygen level might have assisted the oxygenation of ocean waters and eventually the diversification of eukaryotes was terminating with the appearance of early animals (FIKE *et al.* 2006; CANFIELD *et al.*

Author's Address: RUMANA YEASMIN[1,2*], DAIZHAO CHEN[2] & JIANGUO WANG[2], [1]Department of Geological Sciences, Jahangirnagar University, Savar, Dhaka-1342, Bangladesh, [2]Key Laboratory of Petroleum Resources Research, Institute of Geology and Geophysics, Chinese Academy of Sciences, Beijing 100029, China. *Email: rychumki@juniv.edu*

2007). But many recent studies disagree with the scenario of subsequent oxygenation of ocean, especially the deeper part, with rise of atmospheric oxygen concentration and it has been shown that the ocean water in the Yangtze Platform was still severe anoxic during the Ediacaran-Cambrian transition (e.g., GOLDBERG *et al.* 2007; GUO *et al.* 2007; CANFIELD *et al.* 2008; WILLE *et al.* 2008). However, the detail structures of ocean redox conditions of the entire Yangtze Platform remain ambiguous, despite these extensive studies on the significant oceanic geochemical changes around the early Cambrian. Therefore, to mitigate this inconsistency, it is necessary to re-examine the ocean chemistry during the early Cambrian on a basin scale.

Marine sedimentary sequences of the early Cambrian age are widely deposited throughout different paleoenvironmental settings of the Yangtze Platform including shelf, slope and basinal conditions (ZHU *et al.* 2003; YEASMIN *et al.* 2017). These sedimentary successions are well exposed in several sections where extensive researches have been carried out to comprehend spatial variability of ocean chemistry during the early Cambrian. In this paper, detail major and trace elements chemostratigraphy of the early Cambrian succession of the Longbizui section, western Hunan province has been established and correlated with previously published spatiotemporal geochemical data, for examples, iron specification, sulfur isotope in pyrite and trace element concentrations of the early Cambrian sequences from different depositional water depths to explore the marine redox structure of the entire Yangtze Platform during the early Cambrian. For this purpose, the Shatan section (northern Sichuan; GOLDBERG *et al.* 2007; GUO *et al.* 2007); the Jinsha and Weng'an sections (northwestern Guizhou; JIN *et al.* 2016), the Dingtai profile (Guizhou; XU *et al.* 2012); the Yangjiaping section (northwestern Hunan; FENG *et al.* 2014); the Songtao section (eastern Guizhou; GOLDBERG *et al.* 2007; GUO *et al.* 2007; CANFIELD *et al.* 2008); the Longbizui section (western Hunan; WANG *et al.* 2012a); the Daotuo and Bahung sections (northeastern Guizhou; YEASMIN *et al.* 2017) were considered (Fig. 1).

Geological Settings

The Yangtze platform inherited due to rifting and consequent extension of a late Neoproterozoic rifted basin that was initiated at ca. 820–830 Ma (WANG & LI, 2003). As a consequence, the passive continental margin setting was developed during the Ediacaran–Cambrian (E-C) time (JIANG *et al.* 2011) and intense extensional tectonism and block-tilting (KORSCH *et al.* 1991) resulted in the development of different depositional environments with a wide range of water depths that prevailed along a general present-day northwest-to-southeast axis (STEINER *et al.* 2001) – carbonate platforms (the Dengying Formation and its correlative units) were dominated in the shallower northwest part, surrounded by siliceous Liuchapo Formation of slope-basin environments (Fig. 1; CHEN *et al.* 2009; WANG *et al.* 2012a). During the E-C transition, the studied sections were palaeogeographically located in different depositional settings of the Yangtze Platform, for examples, the Jinsha and Weng'an sections were situated in shelf area, the Shatan, Dingtai and Yangjiaping in the shelf marginal areas of different intra-platform basins, the Daotuo and Songtao in the

carbonate-dominated upper slope of the platform area; the Longbizui in the deeper siliceous-dominated mid-slope, while the Bahuang section was located in the deepest siliceous- dominated basin (Fig. 1).

The shaly sequences of the Niutitang Formation and its correlative units (including Guojiaba Formation; Fig. 2) were deposited all over the carbonate platform, slope to deep basin during the early Cambrian due to transgression and subsequent drowning of the carbonate platforms (e.g., GOLDBERG *et al.* 2007). The lower Niutitang Formation generally consists of a thin basal polymetallic sulfide layer and/or nodular phosphate-rich bed overlain by a thick black shale succession (MAO *et al.* 2002). In the upper part of Niutitang and Guojiaba Formations, a change in lithology is observed regionally, e.g., mudstone and silty mudstone layers at the Jinsha and Weng'an sections; mudstone intercalated with limestone at the Shatan section; silty shale at the Dingtai and Yangjiaping sections; shale intercalated with silty shale/siltstone at the Daotuo section; muddy limestone intercalated with mudstone at the Songtao section; thin dolostone bed overlying by thick mudstone layer at the Longbizui section; and mudstone layer in the Bahuang section.

The Niutitang Formation is overlain by the Jiumenchong Formation in paleo-slope to basinal area which is characterized by alternation of limestones with thin black shale layers, but its shallow water equivalent (i.e., Migxinsi Formation at outer shelf areas) is more carbonate dominant. However, only at the Daotuo and

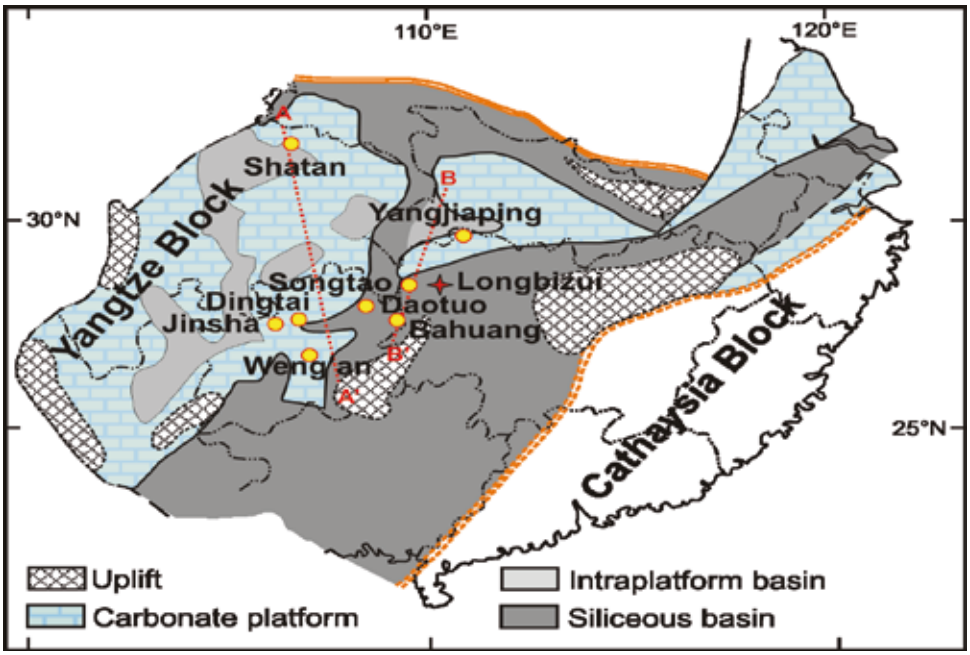

Fig. 1. Sedimentary lithofacies, paleogeographic map of the Yangtze Block during Ediacaran-Cambrian transition (after YEASMIN *et al.* 2017). Disposition of privously studied sections along with the Longbizui are marked. AA′ & BB′ lines are used to construct hypothetical Basin models (Fig. 8)

Longbizui locations the uppermost Bianmachong Formation persists which is dominated by black shales.

Stratigraphic Correlation between Studied Sections

Because of sparse availability of reliable biostratigraphic and radiometric age data, accurate stratigraphic correlation between the early Cambrian sedimentary sequences at different locations on the Yangtze Block is difficult (e.g., ZHU *et al*. 2003; JIANG *et al*. 2012). Fig. 2 shows the lithology and possible correlation between different sections of the Yangtze Block which were located from shelf to deep basin area during the E–C transition (Fig. 1).

The exact position of the E-C boundary (542.0±0.3 Ma; AMTHOR *et al*. 2003) in South China has been highly debated due to the absence of precise radiometric ages. It is traditionally defined by the first occurrence of small shelly fossils (SSF) (CHEN, 1984; QIAN, 1999) and *Micrhystridium*-like acritarchs (YIN, 1997). The SSF assemblage 1 (*Anabarites trisulcantus – Protohertzina unguliformis*) and 2 (*Paraglob-orilus subglobosus – Purella squamulosa*) are abundant in the Shatan section, mainly in phosphorite breccia layers of the upper Kuanchanpu Formation which implies a Fortunian time (STEINER *et al*. 2007). The occurrence of SSF 1 in basal Niutitang Formation of the intrabasinal shelf margin Yangjiaping sections also indicates more or less equivalent time of deposition (ZHU *et al*. 2003; STEINER *et al*. 2007). But owing to the lack of index fossils, the E-C transition cannot be clearly identified in slope to deep basinal deposits based on biostratigraphy. However, the muddy chert with carbonate and phosphorite layers in the uppermost Liuchapo Formation at Songtao is similar to limestone and phosphorite breccia of the Kuanchanpu Formation in the Shatan section (GOLDBERG *et al*. 2007) that signifies the Fortunian age and the E-C boundary is probably located within the Liuchapo Formation of the deeper part of the basin. Moreover, A large negative C_{org} isotopic excursion is noted in the mid Liuchapo Formation at middle slope Longbizui section which substantiates the placement of the E-C boundary there (WANG *et al*. 2012a), as C_{org} isotopic profile has been proven as a reliable tool for the large-scale correlation, particularly in the fossil-deficient E-C successions (KNOLL & WALTER, 1992; KAUFMAN & KNOLL, 1995; ISHIKAWA *et al*. 2008). In deep basinal Bahuang section, the E-C transition is established based on U-Pb zircon age dating which also reveals a lower placement of the boundary in upper-mid Liuchapo Formation (CHEN *et al*. 2015).

In the Yangtze Block, the regional (even intercontinental) phosphogenetic event of the Early Cambrian (SHELDON, 1980; COOK, 1992) is well established since the phosphate-rich layers were deposited all over the carbonate platform and even extended in some basinal areas (Fig. 2). Moreover, several radiometric ages of the basal Niutitang Formation from different sections of the Yangtze Block, e.g., SHRIMP U–Pb zircon age of 532.3±0.7 Ma from volcanic ash bed in Guizhou (JIANG *et al*. 2009); 536.3±5.5 Ma from tuffaceous beds below the Ni–Mo–PGE sulfide layer from western Hunan (CHEN *et al*. 2009); 522.7 ± 4.9 Ma from a tuffaceous bed below the polymetallic (Ni–Mo–PGE) sulfide layer from the Taoying section, northeastern Guizhou (WANG *et al*. 2012b); and most recently the U-Pb zircon age dating

(522–524 Ma) of poly-metallic sulfide layer from the Bahuang and Panmen sections of northeastern Guizhou (CHEN *et al.* 2015), point out the depositional age of Ni–Mo–PGE enriched sulfides layer of the basal Niutitang Formation should be much younger than the E–C boundary, probably from Fortunian to end of Stage 2 of the early Cambrian. However, most part of the Fortunian strata in the Jinsha, Weng'an and Dingtai sections are missing, either due to non-deposition or subaerial erosion associated with a low-angle unconformity between the Dengying and Niutitang Formations (e.g., XU *et al.* 2012; JIN *et al.* 2016).

The different types of trilobite fossils were reported from the black shale layers of lower Niutitang Formation, especially at previous shelf to shelf marginal sections, e.g., trilobites *T. armatus* at the Jinsha and Weng'an sections and *T. niutitangensis* at Dingtai areas including both the Jinsha and Weng'an sections (YANG *et al.* 2003; 2014), point out the depositional age of the black shale layers at beginning of Stage 3. These trilobite species were also abundant in the silty/muddy layers of upper Niutitang Formation at those sections of the previous shelf (JIN *et al.* 2016). Therefore, it has been suggested that the fossil-poor black shale sequence of lower Niutitang Formation in slope to basinal settings supposed to also be placed within the Stage 3 and the overlying silty shale/muddy sequences of upper Niutitang Formation is probably deposited at mid of the Stage 3 (Fig. 2). Numerous fossils have also been preserved including the trilobites *Eoredlichia* and *Wutingaspis* and the bivalved arthropods *Liangshanella* cf. *liangshanensis* and *Hanchungella rotundata* in the upper Guojiaba Formation of Shatan (YIN *et al.* 1999). However, the fossil assemblages dominated by sponge spicules have been found in shales of the upper Niutitang Formation of both Longbizui and Bahuang sections (YEASMIN *et al.* 2017) which are somewhat similar to that in the well known 'Chengjiang Fauna' of Stage 3 (YANG *et al.* 2005).

The trilobite fossils *Mayiella* and *Drepanuroides* in the carbonate dominant Mingxinsi Formation at Jinsha (ZHANG *et al.* 1979); *Hupeidiscus* sp. and *Metaredlichia* sp. in same formation at Weng'an (YANG *et al.* 2003) and also in muddy carbonate layers of the lower Xiaosi member in Songtao section (ZHAO *et al.* 2001); and *Hunanocephalus* sp. at Yangjiaping (YIN *et al.* 1999) are abundant. The appearences of the trilobites *Hubeidiscus orientalis*, *Sinodiscus changyangensis* and *Hunanocephalus* sp. in these sediments indicate roughly late Qiogzhusian to early Changlangpuan age, i.e, within late Stage 3 of early Cambrian (YUAN & ZHAO, 1999; YANG *et al.* 2003). In Daotuo, the occurrences of archaeocynthid in the upper Jiumenchong Formation, and hyolithid and brachiopod in the Bianmachong Formation (YEASMIN *et al.* 2017) suggest the deposition of this sediment at Stage 3 (YIN, 1996; ZHU *et al.* 2007). On the other hand, the basal part of overlying Bianmachong Formation, which generally bears trilobites *Protelenella* and *Chengkouia* in eastern Guizhou, is suggested to correlate with the Canglangpu Stage (YIN, 1996) or the Botoman in Siberia (PENG *et al.* 2012).

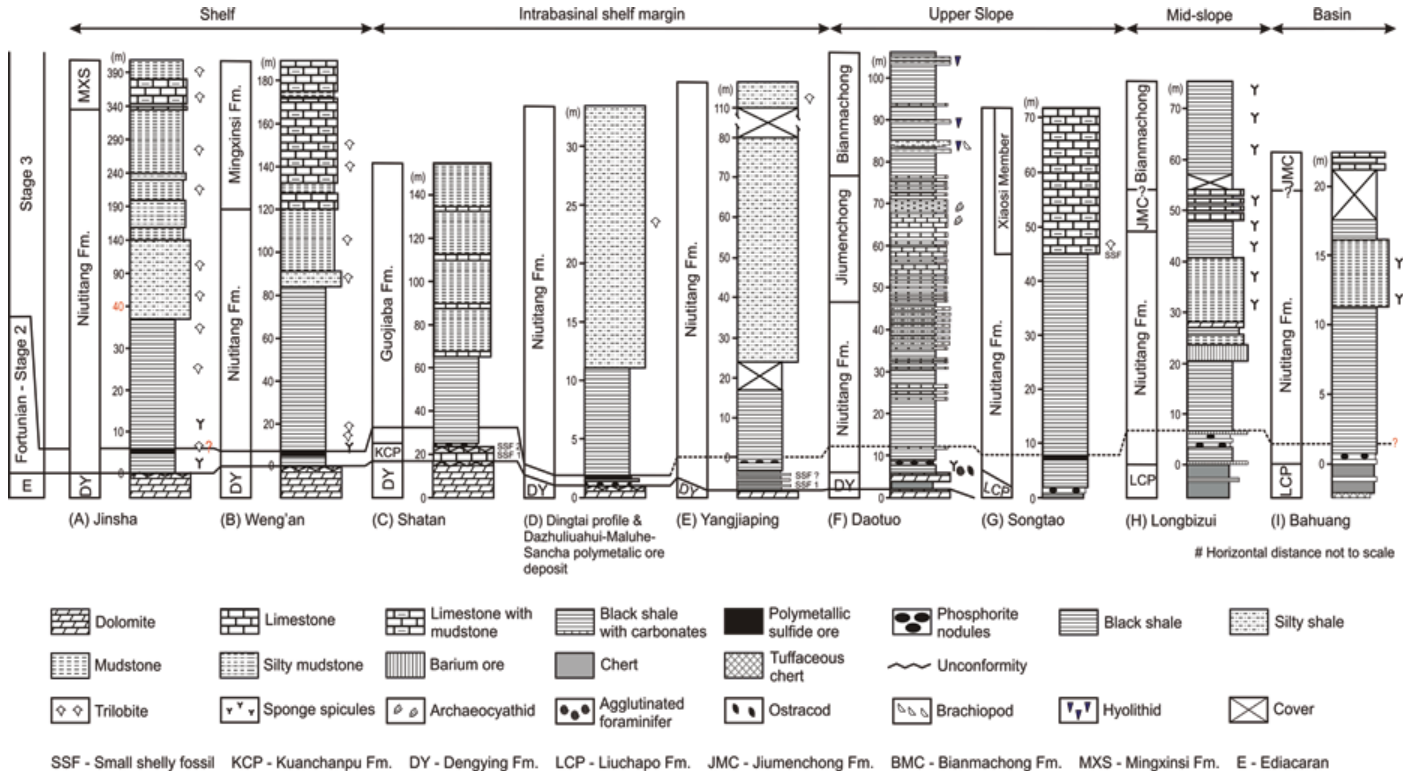

Fig. 2. The stratigraphic correlation of the Early Cambrian strata based on available lithology, fossil records and radiometric age data (see text for description and references). Lithology records for the sections: Jinsha and Weng'an (Jin *et al.* 2016); Shatan (Goldberg *et al.* 2007); Dingtai and adjoining areas (Xu *et al.* 2012); Yangjiaping (Feng *et al.* 2014); Songtao (Goldberg *et al.* 2007); Daotuo, Longbizui and Bahuang (Yeasmin *et al.* 2017).

Methodology

25 shale/mudstone samples from Longbizui were collected and pulverized (<62 m size) in an agate mortar for geochemical analyses. X-ray fluorescence spectrometry (XRF) was used to determine the major elements. Before analysis, oxidized powdered samples were mixed with lithium borate (mixture of 67% $Li_2B_4O_7$ and 33% anhydrous $LiBO_2$) and then melted at 1200°C to make a fusion glass disk of samples which were analyzed using a AXIOS Minerals (PANalytical) spectrometer. Precision of analysis is better than 5%. The samples were also analyzed through an inductively coupled plasma mass spectrometer (Finnigan Element ICP-MS) to determine the concentrations of trace elements such as Ni, Cr, V, Th and U. Precision for all trace elements is estimated to be 5% and accuracy is better than 5% for most elements. The total organic carbon (TOC) in each sample was measured by using a LECO CS-400 analyzer. All analyses were carried out at the Institute of Geology and Geophysics, Chinese Academy of Sciences.

The trace element concentrations are normalized to aluminum (Al) content to avoid the lithological effect and to assess the element concentration from non-aluminosilicate (e.g., biogenic and/or authigenic) sources (CALVERT & PEDERSEN, 1993; VAN DER WEIJDEN, 2002; TRIBOVILLARD *et al.* 2006). These ratios are compared with average shale (AS) vs. Al values (Fig.3) (WEDEPOHL, 1971, 1991).

Result and Discussion

Paleoredox Conditions at Longbizui

Some trace elements, for examples, molybdenum (Mo), vanadium (V) and nickel (Ni) can exhibit distinct sensitivities to different redox conditions to some extent. They are less soluble under oxygen-depleted conditions, resulting syndepositional enrichments in sediments (CALVERT & PEDERSEN, 1993; JONES & MANNING, 1994; POWELL *et al.* 2003) associate with either trace constituents of pyrite or distinct sulfides and/or organic matters (TRIBOVILLARD *et al.* 2006). Therefore, these trace element enrichments, especially their indices such as V/(V+Ni) and V/Cr are used to evaluate relative redox potential for depositional environments. It has been inferred that V/Cr ratios of < 2 signifies oxic seawater, 2 – 4.25 indicates dysoxic conditions, and > 4.25 ratios for suboxic to anoxic conditions (JONES & MANNING, 1994). On the other hand, HATCH & LEVENTHAL (1992) suggested that environments characterized by anoxic conditions lead to sediment V/(V+Ni) ratios of 0.54 – 0.82, while values from 0.46 to 0.60 indicate dysoxic conditions. However, >0.84 values signifies euxinic ocean waters. Another trace element index, i.e., the ratio between actinide metals Th and U is also a good paleoredox indicator (WIGNALL & TWITCHETT, 1996; KIMURA & WATANABE, 2001). The average shale of normal oxidized condition has a Th/U ratio of 3.2 (WEDEPOHL, 1991), but a lower Th/U ratio from 0 to 2 is proposed to indicate an anoxic condition (WIGNALL & TWITCHETT, 1996), because some of U fraction may be precipitated from anoxic pore waters in the course of organic matter (OM) decomposition in sediments during the early diagenesis (GUO *et al.* 2007).

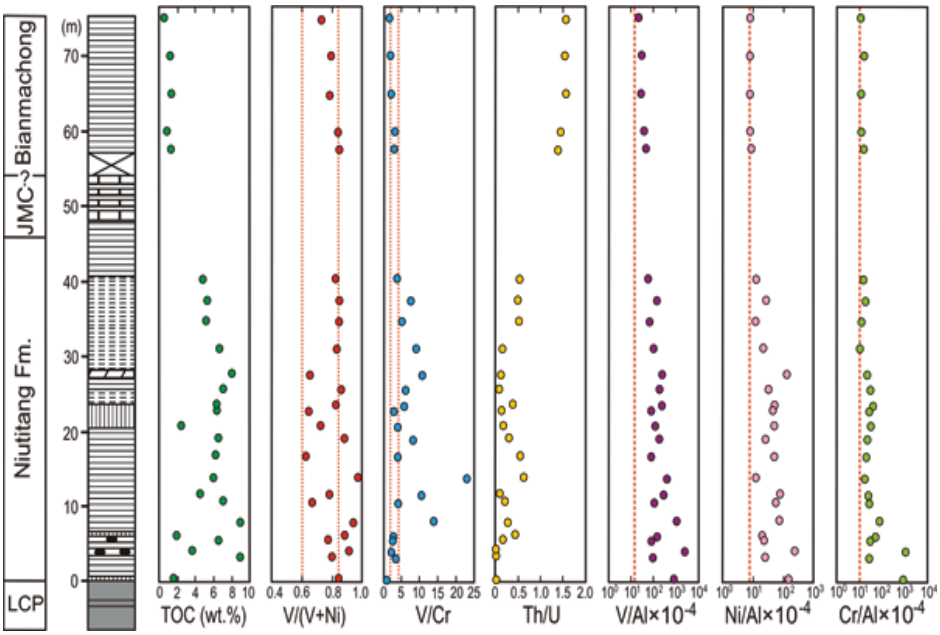

Fig. 3. Vertical variations of multiple geochemical proxies for the Early Cambrian sediments from the Longbizui section. Seawater redox ranges inferred from V/(V + Ni) (HATCH & LEVENTHAL, 1992), V/Cr (JONES & MANNING, 1994) and Th/U ratios (WIGNALL & TWITCHETT, 1996) are marked by the vertical dashed lines. Representative concentrations of trace element ($\times 10^{-4}$) in the average shale vs. Al (V/Al = 14.7, Ni/Al = 7.7, Cr/Al = 10.2; after WEDEPOHL, 1971, 1991) are also marked by the vertical dashed lines.

In shales from the basal Niutitang Formation of the Longbizui section, V and Ni concentrations (i.e., V/Al and Ni/Al ratios) are significantly high, which gradually decrease upward, although much fluctuating particularly in the lower Niutitang Formation (Fig. 3). Among the trace inter-element indices, V/(V+Ni) variations generally follow the patterns of V/Al variations at the studied section (Fig. 3). Their values are greater than 0.6 throughout the studied successions, with some even greater than 0.84, particularly in the basal Niutitang Formation, which reflect variably dysoxic to anoxic conditions throughout the Early Cambrian time with invasion of euxinic waters during deposition of the basal Niutitang Formation. Similarly, V/Cr ratios are mostly higher than 2 (Fig. 3) that also suggest the fluctuating dysoxic to anoxic conditions that gradually evolved into more oxic conditions during deposition of the Bianmachong sediments (i.e., Botomian time).

However, another paleoredox indicator, i.e., Th/U ratios in the Early Cambrian sediments of Longbizui shows relatively low values, thus pointing to an anoxic condition during deposition. But the slight increase of Th/U ratios (up to 1.57) in the Bianmachong Formation suggests a less anoxic, probably suboxic-dysoxic condition during deposition in the Early Botomian, reconciling the scenarios revealed by V/(V+Ni) and V/Cr ratios as documented above.

Early Cambrian Ocean Water Chemistry in the Yangtze Block

Detailed assessment and compilation of iron specification, sulfur isotope and trace element concentrations of the early Cambrian sequences from different parts of the Yangtze Block provides persuasive evidence for temporal and spatial variability of ocean redox conditions on the early Cambrian Yangtze Block (Figs. 4 - 8).

Inferences from Trace Element Concentrations

Together with V and Ni concentrations, Mo is considered one of the best proxies for recognizing the seawater anoxia (especially euxinia) due to strong enrichment in organic-rich facies deposited under seawater sulfate-reducing conditions (DEAN *et al.* 1997; SCOTT & LYONS, 2012). Mo concentrations above the crustal average (2 ppm) and below 25 ppm indicate sediment deposition under non-euxinic conditions, whereas enduring euxinic ocean waters with a link to the open ocean has been suggested if the contents in sediments exceed 100 ppm (SCOTT & LYONS, 2012). However, the intermediate values (25–100 ppm) also reflect euxinia where these relatively low values probably caused by anomalously high sedimentation rates, low concentrations of dissolved Mo in water column, variations in pH of the water column and/or rapid oscillation of euxinic and non-euxinic conditions (SCOTT & LYONS, 2012).

The black shale sequence of the lower Niutitang and lower Guojiaba Formations of the Yangtze Block shows a remarkable enrichments of Mo and most of the samples have concentrations >25 ppm (Fig. 4) which have been attributed to deposition under sulfidic water columns. Mo contents for these sediments range from 30 ppm to 394 ppm (avg. 86 ppm) in the shelf section Jinsha and 21 ppm to 246 ppm (avg. 92 ppm) in the outer shelf Weng'an section. In the lower Niutitang sediments of intrabasinal shelf margin locations, Mo concentrations vary from 2 ppm to 71 ppm (avg. 32 ppm) (Shatan section), 38 ppm to 394 ppm (avg. 171 ppm) (Dingtai) and 45 ppm to 249 ppm (avg. 133 ppm) (Yangjiaping area); whereas 11 ppm to 248 ppm (avg. 99 ppm) Mo contents are found in these sediments of the upper slope Songtao section. In addition, the anoxic to euxinic seawater conditions has been designated by observing V/(V+Ni) values during deposition of the lower Niutitang and Guojiaba formations in the intrabasinal shelf margin to deep basinal areas since the ratios range from 0.54 to 0.82 (Fig. 5). In contrast, the V/Cr ratios in basal part of the Formation of all sections from intrashelf margin to mid slope (Figs. 4 and 5) and Th/U ratios in Shatan section (Fig. 4C) do not show good agreement with V/(V+Ni) values and they suggest less extreme conditions where ocean waters might have been gradually shifted from oxic to anoxic regime. However, high V/(V+Ni) and V/Cr ratios and low Th/U values in the lower Niutitang Formation (above the polymetallic beds) of the shelf margin to upper slope sections of the Yangtze Block imply the persistence of anoxic (occasional euxinic) bottom water conditions (Figs. 4 and 5). In mid slope Longbizui section, the V/(V+Ni) and V/Cr ratios in the entire Niutitang Formation vary in oscillatory fashion where V/(V+Ni) values suggest frequent shifting between euxinic and anoxic conditions, but V/Cr ratios point out fluctuation of dysoxic to

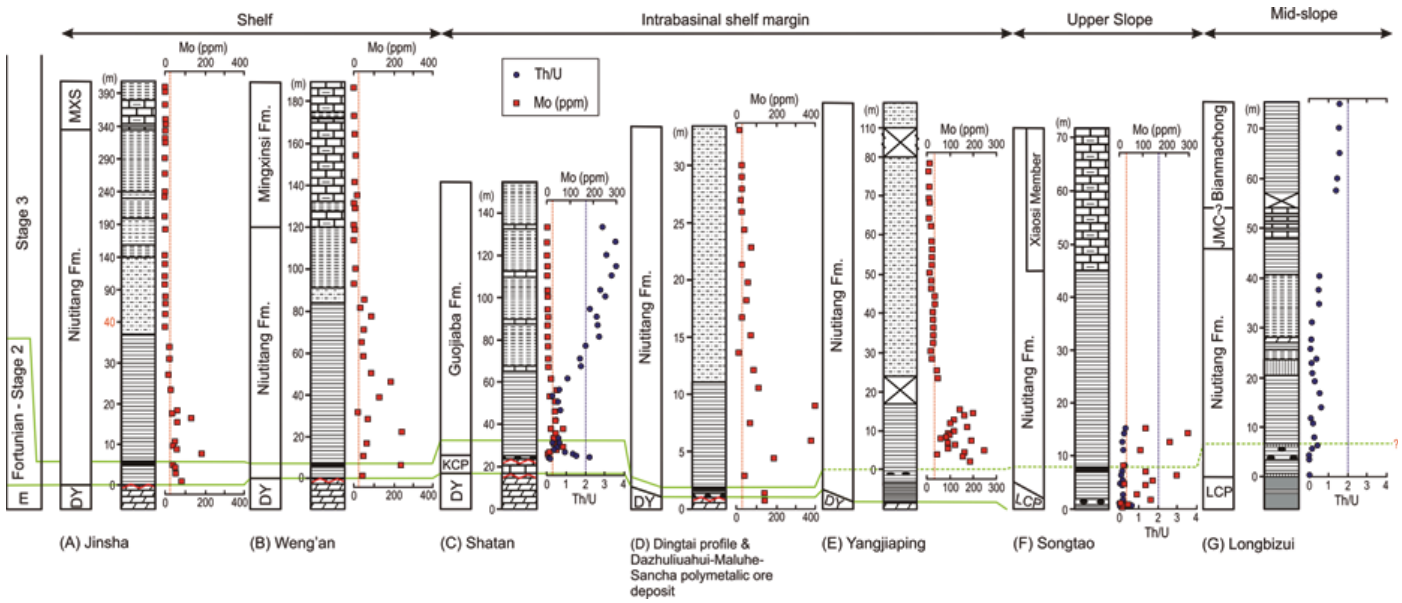

Fig. 4. Chemostratigraphic correlation of Mo (ppm) and Th/U ratios available for the Early Cambrian strata from the Yangtze Block. Data source: Jinsha and Weng'an (Jin *et al* 2016); Shatan and Songtao (Guo *et al*. 2007); Dingtai and adjoining areas (Xu *et al*. 2012); Yangjiaping (Feng *et al*. 2014); and Longbizui (this study). The vertical dashed lines of Mo (red) and Th/U (black) represent boundary values for differentiating alternate redox conditions; detailed on these boundary values can be found in text.

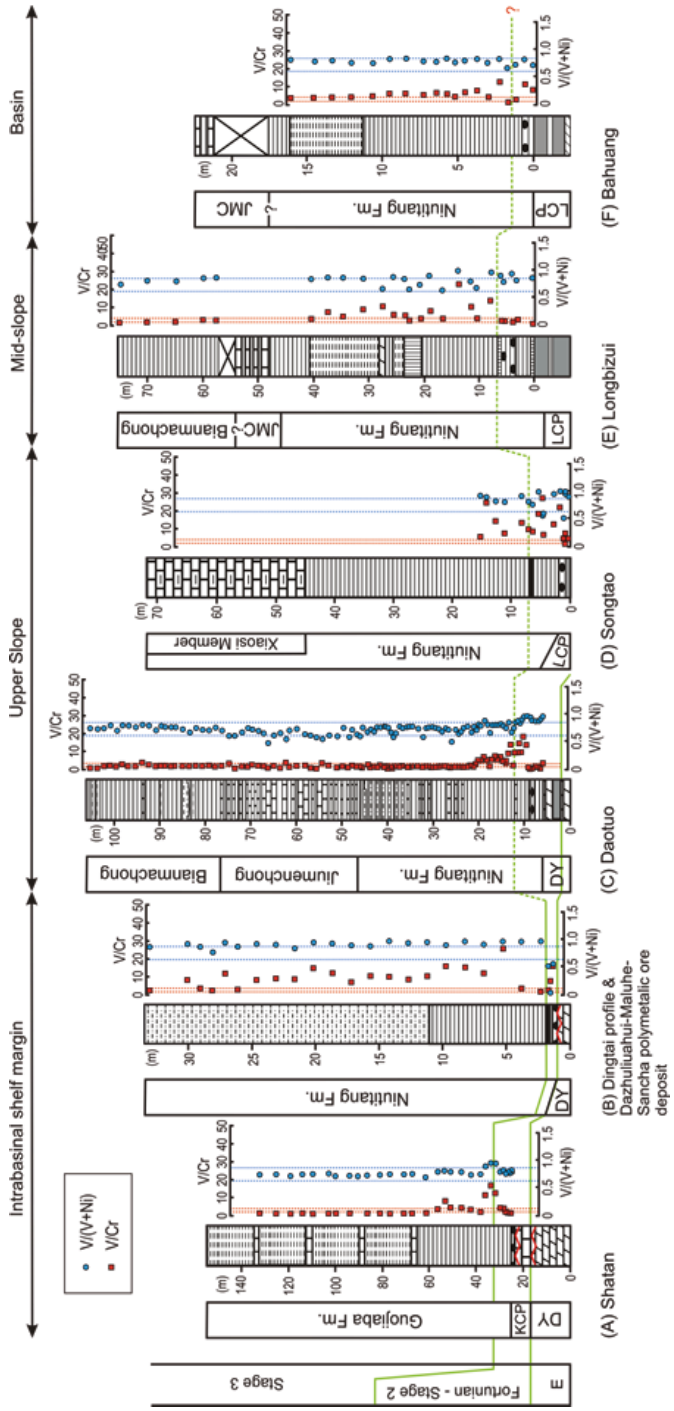

Fig. 5. Chemostratigraphic correlation of trace elements data available for the Early Cambrian strata from the Yangtze Block. Data source: Shatan and Songtao (GUO *et al.* 2007); Dingtai and adjoining areas (XU *et al.* 2012); Yangjiaping (FENG *et al.* 2014); Daotuo and Bahuang (YEASMIN *et al.* 2017) and Longbizui (this study). The vertical dashed lines of V/(V+Ni) (blue) and V/Cr (red) represent boundary values for differentiating alternate redox conditions.

anoxic conditions (Fig. 5E). The V/(V+Ni) and V/Cr ratios in all over the Niutitang Formation at Bahuang section (Fig. 5F) suggest predominance of overall anoxic waters in deep basin, although the basin waters progressively turned into less anoxic (or dysoxic) conditions at the termination of the Niutitang time.

After atrocious anoxic-euxinic conditions, a significant change in ocean water conditions with changes of lithology has been observed in the shelf area of Yangtze Block as low Mo concentrations specify annihilation of euxinic ocean (Fig. 4A and B). Furthermore, low Mo contents coupled with low V/Cr (< 2) and high Th/U (> 2) ratios in the upper Guojiaba Formation in the Shatan section signify rapid shifting to oxic condition, although the V/(V+Ni) values suggest continuation of anoxic condition (Fig. 4C and 5A). These paradoxical hints of paleoredox conditions during deposition of the upper Niutitang are probably the result of several factors such as proportion of riverine influx, types and relative amounts of organic matters, degrees of oceanic mixing, and so on, which significantly affect the trace element concentrations within basin waters (RIMMER, 2004).

However, the trace element indices from the upper Niutitang of Dingtai section (Fig. 5B) indicates the continuation of anoxic conditions in other intrabasinal shelf areas, and the Mo contents in these sediments (Fig. 4D) including another shelf marginal section, i.e., Yangjiaping (Fig. 4E), shows that the anoxic bottom water was persistently fluctuated from euxinic to non-euxinic environments. In contrast, fluctuating anoxic and dysoxic (even occasional oxic) conditions are inferred at that time from trace element indices of the upper Niutitang sediments in relatively deep water upper slope to mid slope settings (i.e., the Daotuo and Longbizui sections) (Fig. 5C and E). Such oscillation of anoxic-oxic conditions also continued during deposition of the Jiumenchong Formation as shown by fluctuating V/(V+Ni) (0.48 - 0.75) and V/Cr (0.75 - 3.86) ratios in the upper slope Daotuo section (Fig. 5C), although the oxic condition dominated at that time. However, the slight increase of these values in the Daotuo and Longbiozui sections of the previous Yangtze slope (Fig. Fig. 5C and E) signifies reoccurring of a more stable anoxic–dysoxic ocean waters during Bianmachong time.

Inferences from Iron Speciation

Iron (Fe) speciation, i.e., total Fe (Fe_T) and highly reactive Fe (Fe_{HR}) concentrations in sediments have been widely used in evaluating the ancient ocean redox chemistry owing to the high sensitivity to water column redox conditions (CANFIELD *et al.* 2008; GILL *et al.* 2011; POULTON & CANFIELD, 2011). The Fe_{HR} comprises pyrite (Fe_{py}) and residual Fe-phases, e.g., ferric oxides, magnetite and Fe-carbonates which are also reactive enough to form pyrite if they are exposed to H_2S (POULTON & CANFIELD, 2011). However, the ratio Fe_{HR}/Fe_T usually exceeds 0.38 when sediments are deposited under anoxic waters (RAISWELL & CANFIELD, 1998). But thermal alteration might potentially alter the Fe_{HR} to nonreactive Fe during burial, reducing this threshold value to 0.15 [0.10 (SD)] (RAISWELL *et al.* 2008). Thus, the Fe_{py}/Fe_{HR} ratio in sediments is additionally used to explore the nature of ocean waters. When

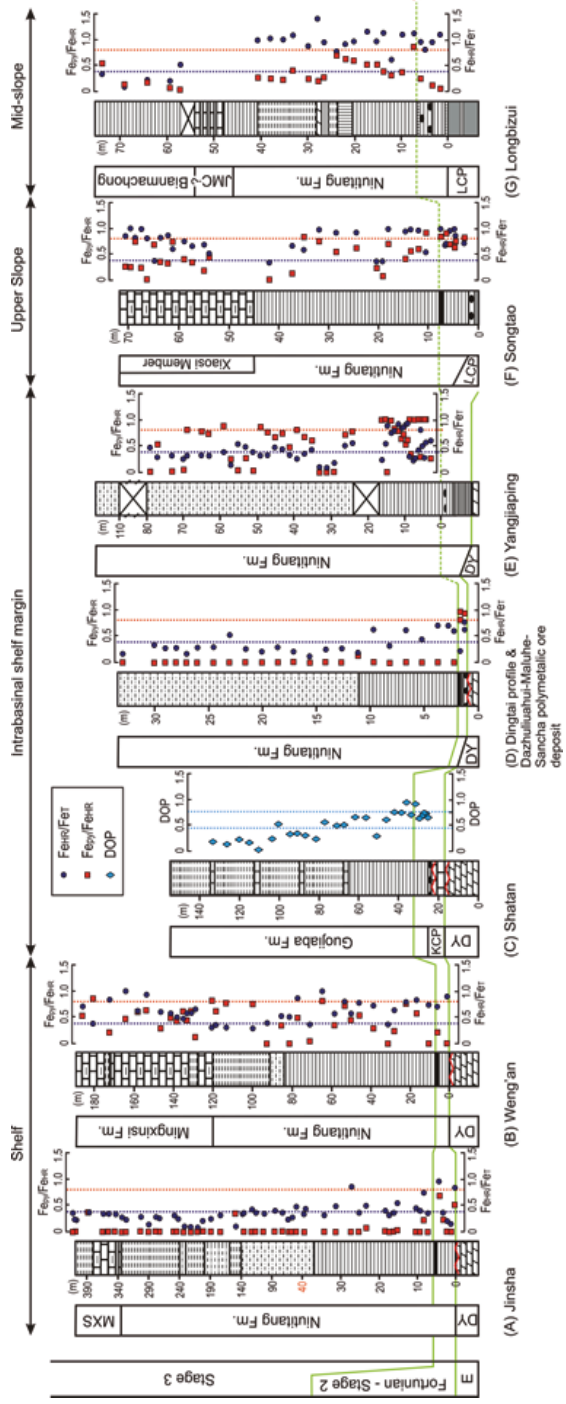

Fig. 6. Chemostratigraphic correlation of iron speciation data available for the Early Cambrian strata from the Yangtze Block. Data source: Jinsha and Weng'an (JIN *et al* 2016); Shatan (GOLDBERG *et al.* 2007); Dingtai and adjoining areas (XU *et al.* 2012); Yangjiaping (FENG *et al.* 2014); Songtao (CANFIELD *et al.* 2008; GOLDBERG *et al.* 2007); Longbizui (WANG *et al.* 2012a). Dashed lines mark at 0.80 of Fe_{py}/Fe_{HR} ratio, 0.38 of Fe_{HR}/Fe_T ratio and 0.45 & 0.75 of DOP, respectively (see text for details).

the ocean water is euxinic due to H_2S production by bacterial sulfate reduction (BSR), most of Fe_{HR} in the system will be altered to Fe_{py}, therefore ratios of Fe_{py}/Fe_{HR} is usually found to be higher than 0.80, whereas the values are lower than 0.80 in ferruginous water columns (POULTON *et al.* 2004; CANFIELD *et al.*, 2008). Another important proxy in this context is the 'degree of pyritization (DOP)', which is the ratio of pyrite (Fe_{py}) over total reactive iron (Fe_R) where Fe_R is the sum of Fe_{py} and HCl-soluble Fe (RAISWELL *et al.* 1988). Thus, euxinic condition seems to appear when DOP values are >0.75 and the DOP of <0.45 indicates an oxic water column (RAISWELL *et al.* 1988). However, intermediate values may reflect dysoxic conditions, but in case of high detrital input to anoxic basin, pyrite formation in water column might be cloaked that decrease the DOP values (ANDERSON & RAISWELL, 2004).

Fig. 6 summarizes the iron speciation data available for the sedimentary sequences in different sections of the Yangtze Block with different water depths during early Cambrian. Most of samples from black shale dominated lower Niutitang Formation of the Yangtze Block have relatively high Fe_{HR}/Fe_T ratios (>0.38), suggesting persistent of ferruginous bottom waters during depositions; except in previous shelf Jinsha location where the variable Fe_{HR}/Fe_T ratios reflect fluctuating oxic to ferruginous waters (Fig. 6). But high (mostly >0.80) Fe_{py}/Fe_{HR} ratios in the basal Niutitang Formation including the polymetallic Mo–Ni–PGE sulfide ore and/or phosphate-rich layers at Yangjiaping, Dingtai and Songtao areas (Fig. 6D - F), suggest that the euxinic event was apparently triumphed over these relatively shallow water part of the Yangtze Block during the earliest Cambrian. However, in previous mid-slope Longbizui section, only two samples in the nodular phosphate-rich shale bed at base of Niutitang Formation have high Fe_{py}/Fe_{HR} (>0.80) (Fig. 6G), indicating a temporarily punctuated sulfidic episode in the earliest Cambrian. The euxinic condition was not prominent in open ocean during the deposition of the black shale since the Fe_{py}/Fe_{HR} ratios are relatively low (<0.8), whereas episodic exaggerations of euxinic waters within ferruginous ocean have been noted by observing variable Fe_{py}/Fe_{HR} ratios in shales of some semi-enclosed intrabasinal shale marginal areas, for example, and Yangjiaping (Fig. 6D). However, low Fe_{py}/Fe_{HR} and Fe_{HR}/Fe_T ratios in some of these black shale samples might also be caused by oxidation of pyrite during weathering after exposure and/or deposition of these shales within iron-limited system (FENG *et al.* 2014).

During deposition of mud dominant upper Niutitang Formation, the ocean water condition was variable from oxic to anoxic (even euxinic) in different part of the Yangtze block. The Fe_{HR}/Fe_T values are low in upper Niutitang silty shales of Jinsha, Weng'an and Dingtai areas (Fig. 6A, B and D), suggesting dominance of oxic waters during deposition. But the Fe_{py}/Fe_{HR} ratios are not analogous with Fe_{HR}/Fe_T in these rocks of Weng'an section (Fig. 6B), suggesting probable diagenetic formation of pyrites in sediments. However, these ratios are variable and rises stratigraphically in an oscillatory fashion in other locality of intrabasinal shelf margins, i.e., in Yangjiaping (Fig. 6E) where the water columns were probably less anoxic to oxic in general but sometimes oscillated to euxinic and ferruginous conditions. On the other hand, during the deposition of muddy limestone of Xiaosi Member at the upper slope

the Songtao and mudstone dominated upper Niutitang Formation at mid slope Longbizui section the ferruginous condition was still persistent which is suggested by high Fe_{HR}/Fe_T ratios (Fig. 6F, G). Afterward, these deep ocean waters were promptly transferred into a rather oxygenated ocean during deposition of the Bianmachong Formation as shown by low Fe_{HR}/Fe_T ratios in Longbizui section (Fig. 6G). But high Fe_{HR}/Fe_T (0.38–1.00) and variable Fe_{py}/Fe_T (0.13–0.85) in sediments of the Mingxinsi Formation at outer shelf Weng'an section (Fig. 6B) indicates dominantly ferruginous conditions which is not supported by Mo concentration in these sediments (Fig. 4B). However, carbonate dilution effects could cause such ambiguous concentrations in the Mingxinsi sediments (JIN *et al.* 2016).

The DOP values were collected only from the intrabasinal shelf margin Shatan section where those values from the black shales of the lower Guojiaba Formation vary from 0.29 to 0.93 (Fig. 6C), signifying the fluctuating redox conditions from dysoxic to anoxic-euxinic waters and they were most likely deposited within or just below a ferruginous chemocline. The values decrease progressively (mostly <0.5) in the upper Guojiaba Formation of this section where limestone layers were frequently deposited within the black shales (Fig. 2). The low DOP and sedimentary evolution point out a subsequent oxygenation of the ocean waters at inner shelf areas during deposition of the upper Guojiaba Formation.

Sulfur Isotopic Composition of Pyrite ($\delta^{34}S_{py}$)

The sulfur isotopic composition in pyrite to some extent depends on the initial abundance of sulfate as well as sulfur isotopic composition of ambient seawater. This isotopic composition in seawater varies throughout the geologic time (SHEN *et al.* 2001). During Archean, the ocean water had low sulfate concentration due to lack of oxidation on continents (HABICHT *et al.* 2002) where $\delta^{34}S_{sulfate}$ values were about +4‰ and the value increased to +32‰ at the E-C transition (STRAUSS, 2004). Later during Phanerozoic, continental oxidation and weathering provided sulfate to ocean (STRAUSS, 2004).

The sulfur isotopic compositions of pyrite within the black shale layers of the lower Niutitang Formation are variable (Fig. 7) and range from -12 to 39.4‰ (mean 13.5‰) in the Jinsha section, from 1.7 to 17.5‰ (mean 8.3‰) in the Yangjiaping, from -5 to 27.0‰ (mean 8.6‰) in the Songtao, and 10.7 to 27.4‰ (mean 19.5‰) in the Longbizui section. A similar chemostratigraphic trend is observed in the black shale sequences of these sections where $\delta^{34}S_{py}$ values first shows discrepancy in basal part and then increase towards the top (Fig. 7D-F), though $\delta^{34}S_{py}$ values of the upper part of the black shale strata shows slightly declining trend in the Jinsha location (Fig. 7A). But in the Shatan section, a quite opposite trend is observed where $\delta^{34}S_{py}$ values are low and mostly show negative values (up to -16.2‰) in the upper most part of black shale layer of the Guojiaba Formation (Fig. 7C), whereas the $\delta^{34}S_{py}$ values of the Weng'an section are highly variable through the lower Niutitang sequence (Fig. 7B). These observations suggest the spatial heterogeneity of $\delta^{34}S_{py}$ in ocean waters of the entire Yangtze Block during the early Cambrian (e.g., FENG *et al.* 2014; JIN *et al.* 2016). However, considering the $\delta^{34}S_{sulfate}$ values of Ediacaran-

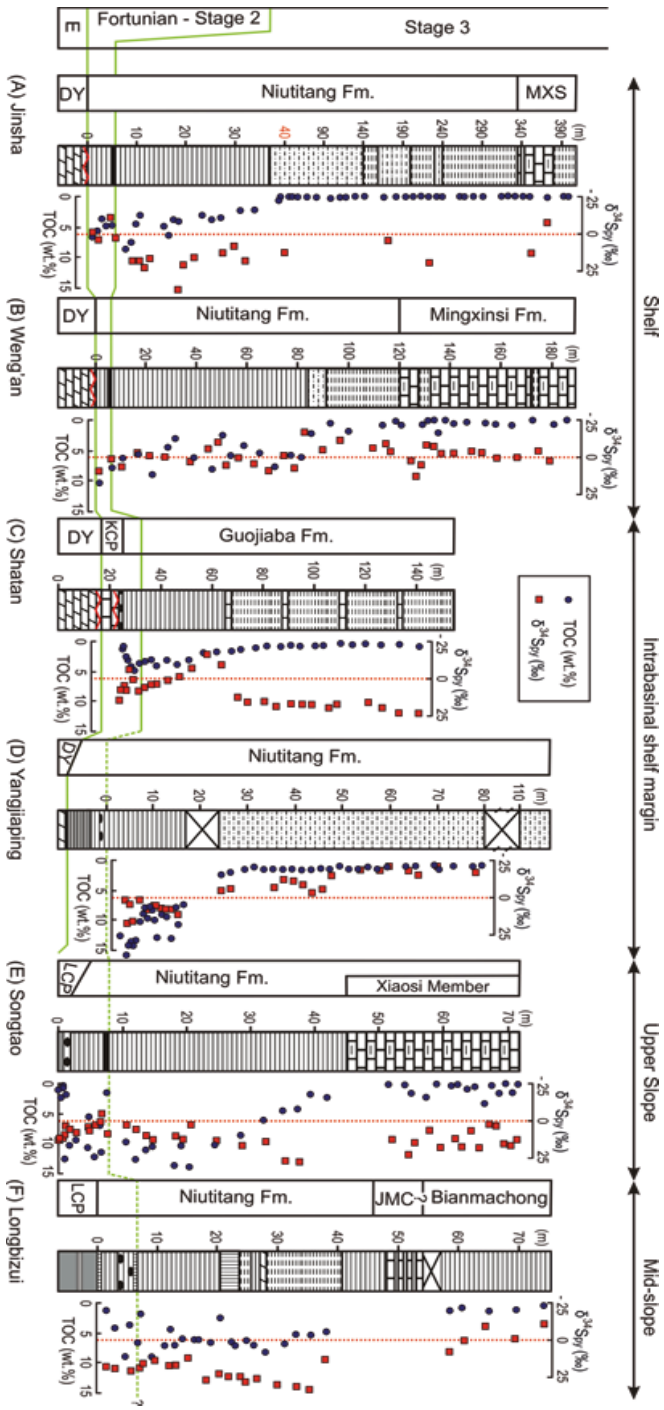

Fig. 7. Composite chemostratigraphy with total organic carbon (TOC) and S-isotopic composition of sedimentary pyrite data for the Early Cambrian strata from the Yangtze Block. Data sources: Jinsha and Weng'an (Jin *et al.* 2016); Shatan and Songtao (Goldberg *et al.* 2007); Yangjiaping (Feng *et al.* 2014); Longbizui (Wang *et al.* 2012a).

Cambrian coeval seawater (25 to 35‰; STRAUSS, 1997), these relatively low positive values in basal Niutitang indicate a relatively high sulfate contents in seawaters during deposition all over the Yangtze Block and the concentrations became variable during deposition of the upper part of the black shale sequences, except in deeper parts of the basin where sulfate concentrations were consistently low, as $\delta^{34}S_{py}$ values are generally higher for those deep-water samples (Fig. 7E-F). Therefore, it is evident that the development of euxinic waters in shallow shelf which might be sustained up to the upper slope water. Such lateral gradient in ocean water chemistry has also been inferred for the Ediacaran Doushantuo Formation in the Yangtze Platform when the low sulfate ocean had been feed through riverine sulfate flux (LI *et al.* 2010). The recurrence of heterogeneous seawater sulfate concentrations during deposition of the lower Niutitang and Guojiaba Formations in the Yangtze Block might also be related to the sources of sulfate. Relatively high sulfates in $\delta^{32}S$ were probably dominant in the near shore shallow shelf close to the riverine sources, whereas low and depleted in $\delta^{32}S$ concentrations prevailed in the deeper part of the basin far away from the sources (LI *et al.* 2010; POULTON *et al.* 2010). In addition, the total organic carbon (TOC) contents in these sediments are relatively high, such as in Jinsha TOC contents vary from 3.7 to 8.6 wt.% (avg. 5.9 wt.%), in Weng'an from 5.5 to 10.2 wt.% (avg. 7.7 wt.%), in Shatan from 0.9 to 4.9 wt.% (avg. 3.1 wt.%), in Yangjiaping from 7.6 to 15.6 (avg. 10.9 wt.%), in Songtao 1.5 – 13.8 (avg. 8.3 wt.%) and in Longbizui 1.9 – 8.9 (avg. 6.1 wt.%), which indicate elevated flux of organic matters in ocean waters through high bioproductivity, because the increment of TOC contents in sediments is fairly propotional with ocean surface-water bioproductivity, regardless of complications arise with efficient organic recycling, export productivity, delivery to the sediment-water interface and final burial (TRIBOVILLARD *et al.* 2006). Such enrichment of organic carbon from shallow to deep waters suggest that the sulfate availability with isotope composition variance might be the main factor controlling the $\delta^{34}S_{py}$ in the lower Niutitang Formation of the Yangtze Block.

The $\delta^{34}S_{py}$ values gradually increase in silty/muddy layers of the upper Niutitang Formation at shelfal Jinsha location (Fig. 7A) and also in the upper Guojiaba Formation at inner-shelf Shatan section (Fig. 7C), implicating return of low sulfate condition during deposition. However, $\delta^{34}S_{py}$ values display more or less increasing-upward tendency in the upper Niutitang Formation of both the Songtao and Longbizui sections of previous slope settings (Fig. 7E-F), while $\delta^{34}S_{py}$ values decrease abruptly from -4.5 to -20.7‰ during deposition of silty shale of the upper Niutitang Formation at Yangjiaping section that was located in one intrabasinal shelf margin (Fig. 7D). Similar trend is also observed in muddy sediments of the upper Niutitang at outer shelf Weng'an section (Fig. 7B). The negative $\delta^{34}S_{py}$ values are likely to reflect the largely increased BSR-mediated sulfur isotopic fractionation in some part of the Yangtze Block during deposition of the upper Niutitang (and equivalent upper Guojiaba Formation), where sulfate concentrations probably increased locally due to rapid land exposure, extensive weathering and consequently high river input during a possible sea-level fall (FENG *et al.* 2014). Similar type of decrease in $\delta^{34}S_{py}$ values occurred during deposition of Mingxinsi Formation at

Jinsha (Fig. 7A) and Weng'an (Fig. 7B) sections and also at the time of the Bianmachong deposition at Longbizui (Fig. 7F) which most likely resulted from a rapid increase in sulfate concentrations in ocean waters as a consequence of increased oxygen concentration (HABICHT *et al.* 2002).

Evolution of Redox Conditions during Early Cambrian

Integrated iron-speciation, sulfur isotope and trace element chemistry from the early Cambrian sedimentary sequences in different areas of the Yangtze Block reveal both temporal and spatial diverse ocean water chemistry that points to a highly stratified water columns and heterogeneously redox marine basin at the beginning of the early Cambrian which gradually oxygenated later. Anoxic bottom water conditions were probably prominent in the Yangtze Block during the late Fortunian to Stage 2 where euxinic condition dominated in the shallower part (Fig. 8A, B). The deposition of polymetallic Mo–Ni–PGE sulfide ore bed along the ancient platform margin of the Yangtze Block gives evidence of a provisional enhancement of sulfide-rich water column (JIANG *et al.* 2007; CHEN *et al.* 2009).

The less positive to negative values of $\delta^{34}S_{py}$, variable Fe_{HR}/Fe_T and low Fe_{py}/Fe_{HR} ratios and relatively low Mo concentrations in the lowermost Niutitang shale in shallow shelf area (i.e., Jinsha section) reflect depositions in fluctuating redox conditions from dysoxic to euxinic. But the permanent euxinic condition developed in relatively deeper shelf and possibly extended up to upper slope during the Fortunian-Stage 2 time (Fig. 8A, B). The $\delta^{34}S_{py}$ values in the outer shelf to upper slope the basal Niutitang black shales including the phophate-rich layers display mostly less positive $\delta^{34}S_{py}$ values and the Fe_{py}/Fe_{HR} ratios are generally >0.8 (Figs. 6 and 7) which are consistent with generation of H_2S by bacterial reduction and syngenetic precipitation of pyrites within the water column as well as in sediment pore water. However, the deeper slope to basin waters were perhaps ferruginous during that time as evident from high Fe_{HR}/Fe_T (>0.38) and low Fe_{py}/Fe_{HR} (<0.70) values within the same stratigraphic interval of basal Niutitang that deposited in Longbizui (Fig. 6G). Multiple studies have revealed that the euxinic and ferruginous stratified redox water conditions coexisted frequently in ancient deep oceans, for example, in Precambrian ocean (JOHNSTON *et al.* 2010; POULTON & CANFIELD, 2011). Therefore, under these circumstances it can be presumed that the Precambrian type ocean chemistry persisted possibly in the earliest Cambrian ocean on the Yangtze Block.

The ferruginous waters might have dynamically invaded up to shelf with probable sea-level rise at the beginning of Stage 3 (Fig. 8C, D) and the ferruginous chemocline shifted upward to shelf marginal areas like Weng'an area. The thick black shale sequences had been deposited in this vicious anoxic condition that is suggested by high Fe_{HR}/Fe_T and low Fe_{py}/Fe_{HR} ratios in these shale samples from the outer shelf Weng'an to deep slope Longbizui sections (Fig. 6), which is also indicated by trace element ratios (Fig. 5). Such anoxic condition was prolonged up to the end of the Niutitang time in deep water settings of the Yangtze Block, as suggested by high Fe_{HR}/Fe_T and trace element indices values in the carbonate rich Xiaosi Member at Songtao and also at the upper Niutitang silty/muddy shale at Longbizui and

Bahuang sections (Figs. 5 and 6). In contrast, the stepwise oxygenation of water columns took place in the shallowest waters much earlier (Fig. 8E), probably during the deposition of the black shales of the lower Niutitang. At that time, ocean waters fluctuated to anoxic-dysoxic conditions at first and then evolved to more oxic state, as observed in the Jinsha section.

The oxygenation of deep basin waters was probably started during the deposition of the Bianmachong Formation at the Longbizui section (Fig. 8F). Available Fe_{HR}/Fe_T data from these sediments (Fig. 6G) suggest that the deepest waters in the basin might have been slightly oxygenated, though the trace element indices (Figs. 4G and 5E) indicate the anoxic condition; but their values hint that the anoxia was not as severe as that occurred during the deposition of the Niutitang. However, the decreasing trend in $\delta^{34}S_{py}$ values in Bianmachong sediments at Longbizui (Fig. 7F) and even in Mingxinsi Formation at Jinsha (Fig. 7A) and Weng'an (Fig. 7B) sections probably resulted from a rapid increase in sulfate concentrations in ocean waters as a consequence of increased oxygen concentration (HABICHT *et al.* 2002) that led to enhance the BSR activity in sediment pores just below sediment-water interface.

The ocean water chemistry in different intra-platformal basins of the Yangtze Block generally follows the overall trend of redox shifting from euxinic (and/or ferruginous) to oxic (Fig. 8). The geochemical data, for examples, the gradual decrease in DOP, Mo concentrations and V/Cr ratios, and subsequent changes of less positive-negative-positive values of $\delta^{34}S_{py}$ in the Guojiaba Formations at Shatan reflect that the waters of a large enclosed basin that was situated within the carbonate

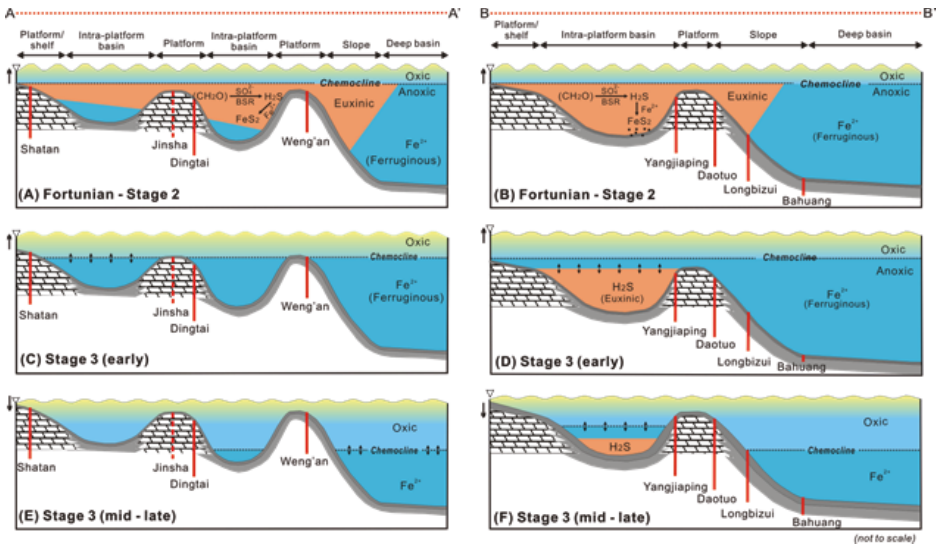

Fig. 8. Hypothetical basin models representing the spatial-temporal evolution of ocean water chemistry in the early Cambrian Yangtze Block. The locations of every section in these models are represented in relative sense, respect to the paleogeography (See Fig. 1 for the location of the cross-sections).

platform at the beginning of the Cambrian (Fig. 1), was rapidly shifted from euxinic waters to oxic, via fluctuating redox conditions from ferruginous to dysoxic (Fig. 8A, C, E). Such condition was coincided perfectly with the changes of water chemistry within previous platformal shelf areas of the Yangtze Block. On the other hand, in one of the semi-enclosed basin where the Dingtai section is located, the redox condition changed according to transformation of water chemistry in outer shelf to upper slope settings. The high Mo concentrations and Fe_{py}/Fe_{HR} ratios in the basal Niutitang at Dingtai (Figs. 4D and 6D) suggest euxinia that gradually changed to ferruginous conditions, and finally from dysoxic to oxic state during deposition of the upper Niutitang, although trace element indices values indicate severe anoxic state during the deposition of the Niutitang Formation at that area (Fig. 5B). In contrast, the Yangjiaping section that was most likely located at shelf margin of another semi-closed intra-platform basin (Fig. 1) where euxinic bottom waters were continued probably for an extended period than in other shelf margin areas of the Yangtze Platform, as shown by high Fe_{py}/Fe_{HR} (≥0.8) (Fig. 6E) which are consistent with strong Mo enrichments in the black shale sequence of the lower Niutitang Formation (Fig. 4E). Later, less anoxic water columns had been established, but highly variable that frequently fluctuate between oxic-ferruginous-euxinic states (Fig. 8F).

Summary

This review article presents a preliminary ocean redox chemistry analysis based on geochemical data such as Fe, S-isotope and trace elements concentrations available in the early Cambrian sedimentary sequences from inner shelf to deep basin areas of the Yangtze Block. These data reveal development of a stratified marine basin in which widespread euxinic waters had been triumphed over inner shelf to slope areas within ferruginous deep waters during the Fortunian-Cambrian Stage 2 time. With sea-level rise, the ferruginous condition became dominant from outer shelf to deep basin, except in one semi-enclosed intra-platformal depression where sulfidic waters dynamically coexisted with the ferruginous waters. This severe anoxic condition began to change in entire Yangtze Block, gradually from shallow shelf to deep basin at the Stage 2-3, probably followed by subsequent regression.

The invasion of severe euxinic waters in shallow shelf was probably main factor for extinction of the Ediacaran fauna and subsequent stepwise bottom water oxygenation further assisted the evolution of new small shelly fauna during the early Cambrian.

Acknowledgements

This study is supported by the National Natural Science Foundation of China (NSFC) through grant Nos. 41472089 and 40839907. The first author acknowledges the PhD scholarship provided by the Organization for Women in Science for the Developing World (OWSD) and Swedish International Development Cooperation Agency (Sida) (Fund Reservation No. 3240237378) for her stay in China.

References

AMTHOR, J.E., GROTZINGER, J.P., SCHRÖDER, S., BOWRING, S.A., RAMEZANI, J., MARTIN, M.W. & MATTER, A., 2003, Extinction of *Cloudina and Namacalathus* at the Precambrian–Cambrian boundary in Oman; *Geology*, **31(5)**, 431– 434.

ANDERSON, T.F. & RAISWELL, R., 2004, Sources and mechanisms for the enrichment of highly reactive iron in euxinic black sea sediments; *American Journal of Science*, **304**, 203–233.

CALVERT, S.E. & PEDERSEN, T.F., 1993, Geochemistry of Recent oxic and anoxic marine sediments: Implications for the geological record; *Marine Geology*, **113**(1-2), 67 – 88.

CANFIELD, D.E., POULTON, S.W. & NARBONNE, G.M., 2007, Late-Neoproterozoic deep-ocean oxygenation and the rise of animal life; *Science*, **315**, 92–95.

CANFIELD, D.E., POULTON, S.W., KNOLL, A.H., NARBONNE, G.M., ROSS, G., GOLDBERG, T. & STRAUSS, H., 2008, Ferruginous conditions dominated later Neoproterozoic deep-water chemistry; *Science*, **321**, 949–952.

CHEN, P., 1984, Discovery of Lower Cambrian small shelly fossils from Jijiapo, Yichang, West Hubei and its significance; *Professional Papers of Stratigraphy and Palaeontology*, **13**, 49–66.

CHEN, D., WANG, J., QING, H., YAN, D. & LI, R., 2009, Hydrothermal venting activities in the Early Cambrian, South China: Petrological, geochronological and stable isotopic constraints; *Chemical Geology*, **258**(3–4), 168–181.

CHEN, D.Z., ZHOU, X.Q., FU, Y., WANG, J.G. & YAN, D.T., 2015, New U-Pb zircon ages of the Ediacaran-Cambrian boundary in South China; *Terra Nova*, **27**, 62–68.

COOK, P.J., 1992, Phosphogenesis around the Proterozoic-Phanerozoic transition; *Journal of the Geological Society, London*, **149**, 615-620.

DEAN, W.E., GARDNER, J.V. & PIPER, D.Z., 1997, Inorganic geochemical indicators of glacial–interglacial changes in productivity and anoxia on the California continental margin; *Geochimica et Cosmochimica Acta*, **61**, 4507–4518.

FENG, L., LI, C., HUANG, J., CHANG, H. & CHU, X., 2014, A sulfate control on marine mid-depth euxinia on the early Cambrian (ca. 529-521 Ma) Yangtze platform, South China; *Precambrian Research*, **246**, 123–133.

FIKE, D.A., GROTZINGER, J.P., PRATT, L.M. & SUMMONS, R.E., 2006, Oxidation of the Ediacaran ocean; *Nature*, **444**, 744–747.

GILL, B.C., LYONS, T.W., YOUNG, S.A., KUMP, L.R., KNOLL, A.H. & SALTZMAN, M.R., 2011, Geochemical evidence for widespread euxinia in the later Cambrian ocean; *Nature*, **469**, 80–83.

GOLDBERG, T., STRAUSS, H., GUO, Q. & LIU, C., 2007, Reconstructing marine redox conditions for the Early Cambrian Yangtze Platform: Evidence from biogenic sulphur and organic carbon isotopes; *Palaeogeography, Palaeoclimatology, Palaeoecology*, **254**(1–2), 175–193.

GUO, Q., SHIELDS, G.A., LIU, C., STRAUSS, H., ZHU, M., PI, D., GOLDBERG, T. & YANG, X., 2007, Trace element chemostratigraphy of two Ediacaran–Cambrian successions in South China: Implications for organosedimentary metal enrichment and silicification in the Early Cambrian; *Palaeogeography, Palaeoclimatology, Palaeoecology*, **254**(1–2), 194–216.

HABICHT, K.S., GADE, M., THAMDRUP, B., BERG, P. & CANFIELD, D.E., 2002, Calibration of sulfate levels in the Archean ocean; *Science*, **298**, 2372–2374.

HATCH, J.R. & LEVENTHAL, J.S., 1992, Relationship between inferred redox potential of the depositional environment and geochemistry of the Upper Pennsylvanian (Missourian) Stark Shale Member of the Dennis Limestone, Wabaunsee County, Kansas, U.S.A.; *Chemical Geology*, **99**(1–3), 65–82.

ISHIKAWA, T., UENO, Y., KOMIYA, T., SAWAKI, Y., HAN, J., SHU, D., LI, Y., MARUYAMA, S. & YOSHIDA, N., 2008, Carbon isotope chemostratigraphy of a Precambrian/Cambrian boundary section in the Three Gorge area, South China: Prominent global-scale isotope excursions just before the Cambrian Explosion; *Gondwana Research*, **14**(1–2), 193–208.

JIANG, S.-Y., YANG, J.-H., LING, H.-F., CHEN, Y.-Q., FENG, H.-Z., ZHAO, K.-D. & NI, P., 2007, Extreme

enrichment of polymetallic Ni–Mo–PGE–Au in Lower Cambrian black shales of South China: An Os isotope and PGE geochemical investigation; *Palaeogeography, Palaeoclimatology, Palaeoecology*, **254**(1–2), 217–228.

Jiang, S.-Y., Pi, D.-H., Heubeck, C., Frimmel, H., Liu, Y.-P., Deng, H.-L., Ling, H.-F. & Yang, J.-H., 2009, Early Cambrian ocean anoxia in South China; *Nature*, **459**, E5–E6.

Jiang, G., Shi, X., Zhang, S., Wang, Y. & Xiao, S., 2011, Stratigraphy and paleogeography of the Ediacaran Doushantuo Formation (ca. 635–551Ma) in South China; *Gondwana Research*, **19**(4), 831–849.

Jiang, G., Wang, X., Shi, X., Xiao, S., Zhang, S. & Dong, J., 2012, The origin of decoupled carbonate and organic carbon isotope signatures in the early Cambrian (ca. 542–520Ma) Yangtze platform; *Earth and Planetary Science Letters*, **317**–**318**, 96–110.

Jin, C., Li, C., Algeo, T.J., Planavski, N., Cui, H., Yang, X., Zhao, Y., Zhang, X. & Xie, S., 2016, A highly redox-heterogenous ocean in South China during the early Cambrian (~529-514 Ma): Implications for biota-environment; *Earth and Planetary Science Letters,* **441,** 38-51.

Johnston, D. T., Poulton, S. W., Dehler, C., Porter, S., Husson, J., Canfield, D. E. & Knoll, A. H., 2010, An emerging picture of Neoproterozoic ocean chemistry: Insights from the Chuar Group, Grand Canyon, USA; *Earth and Planetary Science Letters,* **290**(1–2), 64–73.

Jones, B. & Manning, D.A.C., 1994, Comparison of geochemical indices used for the interpretation of palaeoredox conditions in ancient mudstones; *Chemical Geology*, **111**(1–4), 111–129.

Kaufman, A.J. & Knoll, A.H., 1995, Neoproterozoic variations in the C-isotopic composition of seawater: stratigraphic and biogeochemical implications; *Precambrian Research*, **73**, 27–49.

Kimura, H. & Watanabe, Y., 2001, Ocean anoxia at the Precambrian-Cambrian boundary; *Geology*, **29** (11), 995–998.

Knoll, A.H. & Walter, M.R., 1992, Latest Proterozoic stratigraphy and Earth history; *Nature*, **356**, 673–678.

Knoll, A.H. & Carroll, S.B., 1999, Early animal evolution: emerging views from comparative biology and geology; *Science*, **284**, 2129–2137.

Korsch, R.J., Mai, H., Sun, Z. & Gorter, J.D., 1991, The Sichuan Basin, southwest China: a Proterozoic (Sinian) petroleum province; *Precambrian Research*, **54**, 45–63.

Li, C., Love, G.D., Lyons, T.W., Fike, D.A., Sessions, A.L. & Chu, X., 2010, A stratified redox model for the Ediacaran ocean; *Science*, **328**(5974), 80–83.

Mao, J., Lehmann, B., Du, A., Zhang, G.D., Ma, D.S., Wang, Y.T., Zeng, M.G. & Kerrich, R., 2002, Re–Os dating of polymetallic Ni–Mo–PGE–Au mineralization in Lower Cambrian black shales of South China and its geologic significance; *Economic Geology*, **97**, 1051-1061.

Narbonne, G.M., 2005, The Ediacara Biota: Neoproterozoic origin of animals and their ecosystems; *Annual Review of Earth and Planetary Sciences*, **33**(1), 421–442.

Peng, J., Zhao, Y. & Sun, H., 2012, Discovery and significance of Naraoia from the Qiandongian (lower Cambrian) Balang Formation, Eastern Guizhou, South China; *Bulletin of Geosciences*, **87**(1),143-150.

Poulton, S.W., Fralick, P.W. & Canfield, D.E., 2004, The transition to a sulphidic ocean –1.84 billion years ago; *Nature*, **431**, 173–177.

Poulton, S.W., Fralick, P.W. & Canfield, D.E., 2010, Spatial variability in oceanic redox structure 1.8 billion years ago; *Nature Geoscience*, **3**, 486–490.

Poulton, S.W. & Canfield, D.E., 2011, Ferruginous conditions: a dominant feature of the ocean through Earth's history; *Elements*, **7**, 107–112.

Powell, W.G., JOhnston, P.A. & Collom, C.J., 2003, Geochemical evidence for oxygenated bottom waters during deposition of fossiliferous strata of the Burgess Shale Formation; *Palaeogeography, Palaeoclimatology, Palaeoecology*, **201**(3–4), 249–268.

Qian, Y., 1999, *Taxonomy and biostratigraphy of small shelly fossils in China*, Science Press, Beijing, 247 p.

Raiswell, R. & Canfield, D.E., 1998, Sources of iron for pyrite formation in marine sediments; *American*

Journal of Science, **298**, 219–245.

RAISWELL, R., BUCKLEY, F., BERNER, R.A. & ANDERSON, T.F., 1988, Degree of pyritization of iron as a paleoenvironmental indicator of bottom-water oxygenation; *Journal of Sedimentary Research*, **58**, 812–819.

RAISWELL, R., NEWTON, R., BOTTRELL, S.H., COBURN, P.M., BRIGGS, D.E.G., BOND, D.P.G. & POULTON, S.W., 2008, Turbidite depositional influences on the diagenesis of Beecher's Trilobite Bed and the Hunsrück Slate; sites of soft tissue pyritization; *American Journal of Science*, **308**, 105–129.

RIMMER, S.M., 2004, Geochemical paleoredox indicators in Devonian–Mississippian black shales, Central Appalachian Basin (USA); *Chemical Geology*, **206**(3–4), 373–391.

SCOTT, C., LYONS, T.W., BEKKER, A., SHEN, Y., POULTON, S.W., CHU, X. & ANBAR, A.D., 2008, Tracing the stepwise oxygenation of the Proterozoic ocean; *Nature*, **452**, 456–459

SCOTT, C. & LYONS, T.W., 2012, Contrasting molybdenum cycling and isotopic properties in euxinic versus non-euxinic sediments and sedimentary rocks: refining the paleoproxies; *Chemical Geology*, **324–325**, 19–27.

SHELDON, R.P., 1980, Episodicity of phosphate deposition and deep ocean circulation-A hypothesis: In: Y.K. BENTOR (ed.) Marine Phosphorites—Geochemistry, Occurrence, Genesis; *SEPM Special Publication,* **29**, 239-247.

SHEN, Y., BUICK, R. & CANFIELD, D.E., 2001, Isotopic evidence for microbial sulphate reduction in the early Archaean era; *Nature,* **410**, 77–81.

STEINER, M., WALLIS, E., ERDTMANN, B.-D., ZHAO, Y. & YANG, R., 2001, Submarine-hydrothermal exhalative ore layers in black shales from South China and associated fossils – insights into a Lower Cambrian facies and bio-evolution; *Palaeogeography, Palaeoclimatology, Palaeoecology,* **169**, 165–191.

STEINER, M., LI, G., QIAN, Y., ZHU, M. & ERDTMANN, B.-D., 2007, Neoproterozoic to Early Cambrian small shelly fossil assemblages and a revised biostratigraphic correlation of the Yangtze Platform (China); *Palaeogeography, Palaeoclimatology, Palaeoecology*, **254**(1–2), 67–99.

STRAUSS, H., 2004, 4 Ga of seawater evolution: evidence from the sulfur isotopic composition of sulfate: In: J.P., AMEND, K.J., EDWARDS & T.W., LYONS (eds.) *Sulfur Biogeochemistry-Past and Present*; *GSA Special Papers,* **379**, 195–205.

STRAUSS, H., VIDAL, G., MOCZYDLOWSKA, M. & PACTESNA, J., 1997, Carbon isotope geochemistry and palaeontology of Neoproterozoic to early Cambrian siliciclastic successions in the East European Platform, Poland; *Geological Magazine,* **134**(1), 1–16.

TRIBOVILLARD, N., ALGEO, T.J., LYONS, T. & RIBOULLEAU, A., 2006, Trace metals as paleoredox and paleoproductivity proxies: An update; *Chemical Geology*, **232**(1–2), 12–32.

VAN DER WEIJDEN, C.H., 2002, Pitfalls of normalization of marine geochemical data using a common divisor; *Marine Geology,* **184**(3–4), 167–187.

WANG, J. & LI, Z.-X., 2003, History of Neoproterozoic rift basins in South China: implications for Rodinia break-up; *Precambrian Research*, **122**(1–4), 141–158.

WANG, J., CHEN, D., YAN, D., WEI, H. & XIANG, L., 2012a, Evolution from an anoxic to oxic deep ocean during the Ediacaran–Cambrian transition and implications for bioradiation; *Chemical Geology*, **306–307**, 129–138.

WANG, X., SHI, X., JIANG, G. & ZHANG, W., 2012b, New U–Pb age from the basal Niutitang Formation in South China: Implications for diachronous development and condensation of stratigraphic units across the Yangtze platform at the Ediacaran–Cambrian transition; *Journal of Asian Earth Sciences,* **48**, 1–8.

WEDEPOHL, K.H., 1971, Environmental influences on the chemical composition of shales and clays: In: L.H., AHRENS, F., PRESS, S.K., RUNCORN, H.C., UREY (eds.) *Physics and chemistry of the Earth,* Oxford, 305–333.

WEDEPOHL, K.H., 1991. The composition of the upper Earth's crust and the natural cycles of selected metals: In: E., MERIAN (ed.) *Metals and their compounds in the environment,* VCH-Verlagsgesellschaft, Weinheim, 3–17.

Wignall, P.B. & Twitchett, R.J., 1996, Oceanic anoxia and the end Permian mass extinction; *Science,* **272**, 1155–1158.

Wille, M., Nägler, T.F., Lehmann, B., Schröder, S. & Kramers, J.D., 2008, Hydrogen sulphide release to surface waters at the Precambrian/Cambrian boundary; *Nature,* **453**(196), 767–769.

Xu, L.G., Lehmann, B., Mao, J.W., Nagler, T.F., Neubert, N., Bottcher, M.E. & Escher, P., 2012, Mo isotope and trace element patterns of Lower Cambrian black shales in South China: multi-proxy constraints on the paleoenvironment; *Chemical Geology*, **318**, 45–59.

Yang, A., Zhu, M., Zhang, J. & Li, G., 2003, Early Cambrian eodiscoid trilobites of the Yangtze Platform and their stratigraphic implications; *Progress in Natural Science*, **13**, 861–866.

Yang, X., Zhu, M., Zhao, Y. & Wang, Y., 2005, Cambrian sponge assemblages from Guizhou; *Acta micropalaeontologica Sinica*, **22**(3), 295–303.

Yang, X.L., Zhao, Y., Wu, W., Zheng, H. & Zhu, Y., 2014, Phragmodictya jinshaensis sp. nov., a hexactinellid dictyosponge from the Cambrian of Jinsha, South China; *GFF*, **136**, 309–313.

Yeasmin, R., Chen, D.Z., Fu, Y., Wang, J., Guo, Z. & Guo, C., 2017, Climatic-oceanic forcing on the organic accumulation across the shelf during the Early Cambrian (Age 2 through 3) in the mid-upper Yangtze Block, NE Guizhou, South China; *Journal of Asian Earth Sciences*, **134**, 365 – 386.

Yin, G.Z., 1996, Division and correlation of Cambrian in Guizhou; *Guizhou Geology*, **13**(2), 115–128. *(In Chinese with English abstract)*

Yin, L., 1997, Precambrian–Cambrian transitional acritarch biostratigraphy of the Yangtze Platform; *Bulletin of National Museum of Natural Science (Taipei),* **10**, 217–231.

Yin, G.Z., He, T.G., Qian, Y. & Xiao, B., 1999, Geological and geographical distribution of SSF, with discussion on Early Cambrian geographical provinces: In: Y., Qian, (ed.) *Taxonomy and biostratigraphy of small shelly fossils in China*, Science Press, Beijing, 234–240.

Yuan, J.L. & Zhao, Y.L., 1999, Subdivision and correlation of Lower Cambrian in south-west China, with a discussion of the age of Early Cambrian series biota; *Acta Palaeontologica Sinica*, **38** (S1), 116–131. *(In Chinese with English abstract).*

Zhang, W.T., Yuan, K.X., Zhou, Z.Y., Qian, Y. & Wang, Z.Z., 1979, Cambrian of southwest China: In: Nanjing Institute of Geology and Palaeontology, Chinese Academy of Sciences (eds.) *Biostratigraphy of Carbonates of Southwest China*, Science Press, 39–107. *(In Chinese with English abstract).*

Zhao, Y.L., Yu, Y.Y., Yuan, J.L., Yang, X.L. & Guo, Q.J., 2001, Cambrian stratigraphy at Huanglian, Guizhou Province, China: reference section for bases of the Nangaoan and Duyunian stages; *Palaeoworld*, **13**, 172–181.

Zhu, M., Zhang, J., Yang, A., Li, G., Steiner, M. & Erdtmann, B. D., 2003, Sinian-Cambrian stratigraphic framework for shallow- to deep-water environments of the Yangtze Platform: an integrated approach; *Progress in Natural Science*, **13**(12), 951–960.

Zhu, M., Strauss, H. & Shields, G.A., 2007, From snowball earth to the Cambrian bioradiation: Calibration of Ediacaran–Cambrian earth history in South China; *Palaeogeography, Palaeoclimatology, Palaeoecology*, **254**(1–2), 1–6.

Accepted 16 June, 2019

ক্যাম্ব্রিয়ানের আদি পর্বে ইয়াংজি ব্লকের (বর্তমান দক্ষিণ চীন) মধ্যাবর্তী সমুদ্র জলের অ্যানক্সিক - অক্সিক বিবর্তন পর্যালোচনা

রুমানা ইয়াছমিন, দাইঝাও চ্যান এবং জিয়ানগুয়ো ওয়াং

সারসংক্ষেপ

ক্যাম্ব্রিয়ানের আদি পর্বে জীবের নাটকীয় বির্বতন ও বিচিত্রতা সম্ভবত সমুদ্র জলের প্রতিনিয়ত রাসায়নিক পরিবর্তনের সাথে সরাসরি যুক্ত ছিল। সেজন্য ক্যাম্ব্রিয়ানের আদি পর্বের কালো শেল সমৃদ্ধ পাললিক শীলাস্তরসমূহ স্তরীভূত হওয়ার সময়কার মহাসাগরীয় জলের রসায়ন ব্যাপকভাবে অধীত বিষয়, তবে এখনও বিতর্কিত। প্রকাশিত ভূরাসায়নিক তথ্যের উপর ভিত্তি করে ক্যাম্ব্রিয়ানের আদি সময়কার ইয়াংজি ব্লকের মহাসমুদ্রের জলের রসায়নিক পরিবেশের চিত্র নির্মাণের চেষ্টা হয়েছে, যা বেসিন স্কেলে তৎকালীন সমুদ্র জলের রসায়নের বিবর্তন বৈচিত্রকে চিত্রিত করে। অভ্যন্তরীণ সেল্ফ থেকে গভীর সমুদ্রের পাললিক শীলার প্রকাশিত লৌহ, সালফার আইসোটোপ ও ট্রেস এলিমেন্টের তথ্য সমন্বয় করে বলা যায় যে ইয়াংজি প্লাটফর্মের গভীর সমুদ্রের পানি ক্যাম্ব্রিয়ান শুরুর সময় অ্যানক্সিক ও ফেরুজেনাস ছিল, এবং ভূমি থেকে ক্ষয়প্রাপ্ত সালফার সরবরাহ বেড়ে যাওয়ায় স্বল্প-সুস্থিত ইউজিনিক জল অগভীর সেল্ফে প্রবেশ করেছিল যা অনেক সময় অভ্যন্তরীণ/উর্ধ্ব স্লোপ পর্যন্ত বিস্তার লাভ করেছিল। পাললিক শীলার সালফাইডে তুলনামূলক হালকা সালফার আইসোটোপের সমৃদ্ধি এই অত্যন্ত স্তরীয় জলস্তম্ভের অস্তিত্ব প্রমান করে, যদিও ইডিয়াকারান-ক্যাম্ব্রিয়ান ট্রানজিশন সময় সমগ্র মহাসাগরীয় জলে সালফেট হ্রাস পেয়েছিল, এবং রিঅ্যাক্টিভ আয়রন সাথে পাললিক শীলার আয়রন সালফাইড ও রেডক্স-সংবেদনশীল ট্রেস উপাদানসমূহের পরিমান বৃদ্ধি পেয়েছিল। মহাসাগরীয় রেডক্স-রসায়ন সম্পর্কিত এই স্তরীয় জলস্তম্ভ সম্ভবত সমুদ্রের উচ্চতা বৃদ্ধির সময় ব্যাপকভাবে বিস্তার লাভ করেছিল, কিন্তু পরবর্তীতে সংকুচিত হতে শুরু করে এবং যখন সমুদ্রের উচ্চতা হ্রাসের সাথে সাথে বেসিনটি বিবর্তিত হওয়া শুরু করে তখন অবশেষে এই স্তরীয় জলস্তম্ভ বিলীন হয়ে যায়।